Single-Shot Surface Profiling by Local Model Fitting

Masashi Sugiyama (sugi@cs.titech.ac.jp)
Department of Computer Science, Tokyo Institute of Technology
2-12-1-W8-74, O-okayama, Meguro-ku, Tokyo, 152-8552, Japan

Hidemitsu Ogawa (hidemitsu-ogawa@kuramae.ne.jp)
Toray Engineering Co., Ltd.
1-1-45 Oe, Otsu, Shiga, 520-2141, Japan

Katsuichi Kitagawa (Katsuichi_Kitagawa@toray-eng.co.jp)
Toray Engineering Co., Ltd.
1-1-45 Oe, Otsu, Shiga, 520-2141, Japan

Kazuyoshi Suzuki (Kazuyoshi_Suzuki@toray-eng.co.jp)
Toray Engineering Co., Ltd.
1-1-45 Oe, Otsu, Shiga, 520-2141, Japan

Abstract

We propose a new surface profiling algorithm called the local model fitting (LMF) method. LMF has the following advantages. It is a single-shot method which employs only a single image, so it is fast and robust against vibration. LMF does not require a conventional assumption of smoothness of the target surface in the band-limit sense, but we instead assume that the target surface is locally constant. This enables us to recover sharp edges on the surface. LMF employs only local image data, so objects covered with heterogeneous materials can also be measured. The LMF algorithm is simple to implement and is efficient in computation. Experimental results showed that the proposed LMF method works excellently.

1 Introduction

A standard optical interferometric surface profiler observes the signal $g(x, y)$ of the following form at a position (x, y) on the surface of a target object:

$$g(x, y) = a(x, y) + b(x, y) \cos\left(\phi(x, y)\right), \tag{1}$$

where $a(x, y)$ and $b(x, y)$ are the bias and the amplitude. $\phi(x, y)$ contains the information on the surface profile, which we would like to extract.

The *phase shift method* [1] is a popular and widely-used technique for measuring surface profiles. It estimates $\phi(x, y)$ from image data $\{g_t(x, y)\}_t$ consisting of at least three different phases t:

$$g_t(x, y) = a(x, y) + b(x, y) \cos\left(\phi(x, y) + \pi t/2\right). \tag{2}$$

Typically, such image data with different phases are obtained by carrying out measurement multiple times by changing the relative distance of the reference mirror. When 5 image data $\{g_t(x, y)\}_{t=-2}^{2}$ are observed, tangent of $\phi(x, y)$ can be constructed as

$$\tan\phi(x, y) = \frac{\sin\phi(x, y)}{\cos\phi(x, y)} = \frac{2g_{-1}(x, y) - 2g_1(x, y)}{2g_0(x, y) - g_{-2}(x, y) - g_2(x, y)}. \tag{3}$$

By applying the arctangent operation to the above equation, $\phi(x, y)$ can be recovered. Note that the arctangent operation using the signs of $\cos\phi$ and $\sin\phi$ produces wrapped phase maps in a 2π range. This is usually restored by a *phase-unwrapping* algorithm [2].

Although the phase shift method is known to be able to measure the surface profile accurately, it has two major drawbacks: the measurement speed is not so fast and the high accuracy could be degraded by disturbance such as vibration. These drawbacks are mainly due to the fact that the method needs to observe image data multiple times by changing the relative distance of the reference mirror.

To overcome these problems, surface profiling methods which only require a single image (i.e., 'single-shot') have been proposed, e.g., the *Fourier transform method* [3] and the *spatial phase synchronization method* [4]. The key idea of these methods is to slightly tilt the reference mirror, by which signals with different phases are constructed.

$$g(x, y) = a(x, y) + b(x, y) \cos\left(\phi(x, y) + 2\pi f x\right), \tag{4}$$

where f is the spatial carrier frequency along the x-axis.

The Fourier transform method and the spatial phase synchronization method assume that $\phi(x, y)$ is *smooth* in the band-limit sense as a function of x. Under this assumption, the Fourier transform method extracts $\phi(x, y)$ by applying a high-pass and a shift operations to the observed signal in the frequency domain. The spatial phase synchronization method extracts $\phi(x, y)$ by constructing sine and cosine of $\phi(x, y)$ through low-pass filtering. A common feature of these single-shot methods is that they use integral transforms such as the Fourier transform and high/low-pass filtering. This means that, in principle, these methods require the signal $g(x, y)$ *globally* on the x-domain.

In practice, the above single-shot methods have several drawbacks. First, a rather restrictive assumption of smoothness of the surface profile in the band-limit sense has to be imposed. This makes it impossible to measure the surface profile of an object with sharp steps. Second, integral transforms which are defined for continuous functions can not be exactly computed from discrete image data. Therefore, they should be replaced by discrete transforms, which produces approximation errors. Third, image data obtained globally from the x-domain are needed for estimating the surface profile. The surface of objects we want to measure is often heterogeneous: materials covering the target surface may not be globally identical, which makes the global methods unreliable. Note that the last problem could be avoided by using a windowed transform with small window width, although such a windowed transform produces additional approximation errors.

Another single-shot method, the *spatial phase shift method* [5, 6] requires image data only in a local region. The spatial phase shift method assumes that the reference mirror is tilted so that the observed signal exactly yields

$$g(x,y) = a(x,y) + b(x,y)\cos\left(\phi(x,y) + \pi x/2 + \pi y\right). \tag{5}$$

Although it is not explicitly written in the original paper, $a(x,y)$, $b(x,y)$, and $\phi(x,y)$ are assumed to be constant for neighboring up/down/left/right points. Then, similar to the ordinary phase-shift method, tangent of $\phi(x,y)$ can be constructed as

$$\tan\phi(x,y) = \frac{\sin\phi(x,y)}{\cos\phi(x,y)} = \frac{2g(x-1,y) - 2g(x+1,y)}{2g(x,y) - g(x,y-1) - g(x,y+1)}. \tag{6}$$

Thanks to the locality, the spatial phase shift method does not suffer from the drawbacks of the global methods. However, in practice, tilting the reference mirror so that Eq.(5) is exactly fulfilled may not be possible, and the accuracy is heavily affected by a small error in the angle of the reference mirror.

In this paper, we propose an alternative single-shot surface profiling algorithm, which is algorithmically simple, computationally efficient, and accurate. The proposed method, called the *local model fitting* (LMF) method, is also a local method; LMF works with at minimum one neighboring point. Therefore, it does not suffer from all the problems caused by the globality. Furthermore, LMF can be applied to the tilted reference mirror of any angle, which remarkably contributes to high practicality.

A basic idea of the LMF method is that a parametric model of the local surface profile is fitted to image data, which is detailed in Section 2 and Section 3. We report exemplary results of actual measurement in Section 4, and give concluding remarks in Section 5.

2 General Form of the Local Model Fitting (LMF) Algorithm

In this section, we derive a new surface profiling algorithm called the *local model fitting (LMF)* method.

Here, we tilt the reference mirror in an arbitrary angle. Therefore, our observation model is given by

$$g(x,y) = a(x,y) + b(x,y)\cos\left(\phi(x,y) + 2\pi f_x x + 2\pi f_y y\right), \tag{7}$$

where f_x and f_y are the spatial carrier frequencies along x- and y-axes, respectively. Suppose we have image data $\{g(x_i,y_i)\}_{i=1}^n$ in the vicinity of a point of interest (x_0,y_0). Our goal is to estimate $\phi(x_0,y_0)$ from $\{g(x_i,y_i)\}_{i=1}^n$.

Here we make the following assumption: $a(x,y)$, $b(x,y)$, and $\phi(x,y)$ are constant in the vicinity of (x_0,y_0), i.e., our local model is

$$g(x,y) = a + b\cos\left(\phi + 2\pi f_x x + 2\pi f_y y\right). \tag{8}$$

If the target surface $\phi(x,y)$ is smooth, this assumption can be approximately satisfied by taking the size of the vicinity small enough. On the other hand, this assumption is not fulfilled at discontinuous regions. However, the effect of such errors stay within local regions so the errors do not degrade the overall estimation results (see Section 4 for experimental evaluation). In contrast, the conventional assumption of low-frequenciness of $\phi(x,y)$ affects the entire region even if discontinuity of $\phi(x,y)$ is localized [3, 4].

Suppose we have reasonable estimates of the spatial carrier frequencies f_x and f_y, denoted by $\widehat{f_x}$ and $\widehat{f_y}$, respectively. Such $\widehat{f_x}$ and $\widehat{f_y}$ may be obtained from image data of a flat area. Note that the spatial carrier frequencies f_x and f_y are global quantities which do not depend on the target object and are determined by the (relative) tilting angle of the reference mirror.

Then unknowns in the simplified model (8) are only a, b, and ϕ. We may determine the unknowns by solving the following least-squares problem:

$$(\widehat{a},\widehat{b},\widehat{\phi}) = \operatorname*{argmin}_{(a,b,\phi)} \sum_{i=1}^{n} \left[g(x_i,y_i) - a - b\cos(\phi + 2\pi\widehat{f_x}x_i + 2\pi\widehat{f_y}y_i)\right]^2. \tag{9}$$

However, solving this least-squares problem is cumbersome since the model is non-linear with respect to ϕ. To ease the problem, we employ the following reparameterization:

$$\begin{aligned} &a + b\cos(\phi + 2\pi\widehat{f_x}x + 2\pi\widehat{f_y}y) \\ &\quad = a + b\cos\phi\cos(2\pi\widehat{f_x}x + 2\pi\widehat{f_y}y) - b\sin\phi\sin(2\pi\widehat{f_x}x + 2\pi\widehat{f_y}y) \\ &\quad = a + \xi_c\varphi_c(x,y) + \xi_s\varphi_s(x,y), \end{aligned} \tag{10}$$

where

$$\xi_c = b\cos\phi, \tag{11}$$

$$\xi_s = b\sin\phi, \tag{12}$$

$$\varphi_c(x,y) = \cos(2\pi\widehat{f_x}x + 2\pi\widehat{f_y}y), \tag{13}$$

$$\varphi_s(x,y) = -\sin(2\pi\widehat{f_x}x + 2\pi\widehat{f_y}y). \tag{14}$$

Now we solve the following least-squares problem instead:

$$(\widehat{a}, \widehat{\xi}_c, \widehat{\xi}_s) = \underset{(a,\xi_c,\xi_s)}{\operatorname{argmin}} \sum_{i=1}^{n} \left[g(x_i, y_i) - a - \xi_c \varphi_c(x_i, y_i) - \xi_s \varphi_s(x_i, y_i) \right]^2 . \tag{15}$$

Since the above model is linear with respect to a, ξ_c, and ξ_s, we can analytically obtain the least-squares solutions $\widehat{a}$, $\widehat{\xi}_c$, and $\widehat{\xi}_s$ as

$$\begin{pmatrix} \widehat{a} \\ \widehat{\xi}_c \\ \widehat{\xi}_s \end{pmatrix} = (\boldsymbol{A}^\top \boldsymbol{A})^{-1} \boldsymbol{A}^\top \boldsymbol{g}, \tag{16}$$

where $^\top$ denotes the transpose of a matrix, and

$$\boldsymbol{A} = \begin{pmatrix} 1 & \varphi_c(x_1, y_1) & \varphi_s(x_1, y_1) \\ 1 & \varphi_c(x_2, y_2) & \varphi_s(x_2, y_2) \\ \vdots & \vdots & \vdots \\ 1 & \varphi_c(x_n, y_n) & \varphi_s(x_n, y_n) \end{pmatrix}, \tag{17}$$

$$\boldsymbol{g} = \begin{pmatrix} g(x_1, y_1) \\ g(x_2, y_2) \\ \vdots \\ g(x_n, y_n) \end{pmatrix}. \tag{18}$$

Given $\widehat{\xi}_c$ and $\widehat{\xi}_s$, we can obtain an estimate $\widehat{\phi}$ of the surface profile at (x_0, y_0) by

$$\widehat{\phi}(x_0, y_0) = \arctan(\widehat{\xi}_s / \widehat{\xi}_c) + 2m\pi, \tag{19}$$

where m is an unknown integer. Note that we can determine the value of arctangent upto a 2π range by using the signs of $\cos\phi$ and $\sin\phi$. Since b is always positive, the signs of $\cos\phi$ and $\sin\phi$ could be estimated by the signs of $\widehat{\xi}_c$ and $\widehat{\xi}_s$, respectively (cf. Eqs.(11) and (12)). m may be determined by a phase-unwrapping algorithm [2]. We call the above method *Local Model Fitting (LMF)*.

Thanks to the above least-squares formulation, our solutions $\widehat{a}$, $\widehat{\xi}_c$, and $\widehat{\xi}_s$ are guaranteed to be optimal in the least-squares sense even when $\{g(x_i, y_i)\}_{i=1}^n$ include some measurement noise. Note that employing least-squares fitting in surface profiling itself is not a novel idea. See, e.g., the least-squares formulation of the phase shift method [7].

The LMF algorithm works independently in each local region. Therefore, it is robust against spatial signal deficiencies since the effect of such errors stays within a local region, not propagated globally.

3 Efficient Implementation of LMF Algorithm for Almost Flat Objects

Often an optical surface profiler is used for confirming whether the flat-polished surface is really flat. In this section, we show a variant of the LMF algorithm when the target

surface is known to be almost flat along the x-axis.

Suppose we have equidistance image data along the x-axis:

$$\{g(x_i, y_i) \mid x_i = i, y_i = 0\}_{i=1}^{p}. \tag{20}$$

Then the model does not depend on y, thus our model is reduced to

$$g(i) = a + b\cos\left(\phi + 2\pi\widehat{f}i\right) \quad \text{for } i = 1, \ldots, p. \tag{21}$$

When the target surface is almost flat along the x-axis, the bias a would be globally almost constant. Then a global estimate of a is given by

$$\widehat{a} = \frac{1}{p}\sum_{i=1}^{p} g(i). \tag{22}$$

We implicitly assumed that the above summation extends approximately over one fringe period. This may not be restrictive since typically we have much more fringe periods (see the experiments in Section 4). Now unknowns are only b and ϕ, which are reparameterized as ξ_c and ξ_s in the same way as Eq.(10). Further subtracting $\widehat{a}$ from $g(i)$ yields

$$g_i \equiv g(i) - \widehat{a} = \xi_c c_i - \xi_s s_i, \tag{23}$$

where

$$c_i = \cos(2\pi\widehat{f}i), \tag{24}$$

$$s_i = \sin(2\pi\widehat{f}i). \tag{25}$$

Let us employ k successive local points $\{g_{x+i}\}_{i=0}^{k-1}$ for estimating $\phi(x+(k-1)/2)$, where $x + (k-1)/2$ is the center of the k points $\{x+i\}_{i=0}^{k-1}$. Then the least-squares solutions $\widehat{\xi_c}$ and $\widehat{\xi_s}$ are explicitly expressed in a simpler form:

$$\widehat{\xi_c} = (\alpha_{ss}\alpha_{cg} - \alpha_{cs}\alpha_{sg})/\gamma, \tag{26}$$

$$\widehat{\xi_s} = (\alpha_{cs}\alpha_{cg} - \alpha_{cc}\alpha_{sg})/\gamma, \tag{27}$$

where

$$\alpha_{cc} = \sum_{i=0}^{k-1} c_{x+i}^2, \tag{28}$$

$$\alpha_{ss} = \sum_{i=0}^{k-1} s_{x+i}^2, \tag{29}$$

$$\alpha_{cs} = \sum_{i=0}^{k-1} c_{x+i} s_{x+i}, \tag{30}$$

$$\alpha_{cg} = \sum_{i=0}^{k-1} c_{x+i} g_{x+i}, \tag{31}$$

$$\alpha_{sg} = \sum_{i=0}^{k-1} s_{x+i} g_{x+i}, \tag{32}$$

$$\gamma = \alpha_{cc}\alpha_{ss} - \alpha_{cs}^2. \tag{33}$$

Note that α_{cc}, α_{ss}, and α_{cs} do not depend on the measured value $g(i)$, so they can be computed in advance. Furthermore, γ is expressed as

$$\gamma = \frac{1}{2} \sum_{i,j=0}^{k-1} s_{i-j}^2, \tag{34}$$

which implies that it does not even depend on the location x (i.e., it takes globally the same value). These facts contribute to saving computational costs. Given $\widehat{\xi_c}$ and $\widehat{\xi_s}$, we can estimate ϕ by Eq.(19).

When $k = 2$, i.e., only two neighboring points g_x and g_{x+1} are used for estimating $\phi(x + 1/2)$, a simple calculation yields

$$\widehat{\xi_c} = \tau_c / s_1, \tag{35}$$

$$\widehat{\xi_s} = \tau_s / s_1, \tag{36}$$

where

$$\tau_c = g_x s_{x+1} - g_{x+1} s_x, \tag{37}$$

$$\tau_s = g_x c_{x+1} - g_{x+1} c_x. \tag{38}$$

Therefore, we have

$$\widehat{\phi}(x + 1/2) = \arctan(\tau_s/\tau_c) + 2m\pi. \tag{39}$$

The signs of $\cos\phi$ and $\sin\phi$ could be estimated by the signs of τ_c and τ_s, respectively, since s_1 is typically positive and b is positive.

4 Measurement Results

In this section, we report exemplary results of actual measurement by the LMF algorithm.

We installed the line-wise version of the LMF algorithm given in Section 3 in the optical surface profiler *SP-500* by Toray Engineering Co., Ltd[1], which allows us to simultaneously measure the surface profile of 512 by 480 pixels.

Figure 1-(a) illustrates the surface profile of the target object (Figure 1-(b)–(d) will be explained later). The height of the bumps is 67.7 ± 1.2nm. Note that the local constant assumption of the target surface is heavily violated at the sharp edges of the bumps. So one of the purposes of the experiments here is to investigate the robustness of the proposed LMF algorithm against the violation of the local constant assumption. The wavelength of the light source is 602.92nm, and the reference mirror is tilted so that approximately 10 fringe periods are included in the plotted area. Figure 2-(a) depicts the observed image $g(x, y)$, while Figure 2-(b) depicts the one-dimensional plots of the observed signal at $y = 240$. Note that we also carried out the same experiments with larger numbers of fringe periods upto 30. The results were almost identical, so we omit those results and only report the result with 10 fringe periods.

To investigate the basic characteristics of the LMF algorithm, we first evaluate the performance of line-wise measurement at $y = 240$. Figure 3 depicts the recovered surface profiles. We begin with explaining Figure 3-(a)–(c) which correspond to the cases where the number of neighbors is $k = 2, 5, 10$, respectively. w in the figure captions and the rest of the graphs in Figure 3 will be explained later. Here we determined the estimate $\widehat{f}$ of the spatial carrier frequency so that the base of the object is displayed horizontally. When $k = 2$, the surface profile of the sharp bump can be successfully recovered, although the recovered flat areas are rather noisy. As k increases, noise reduction effects appear and the flat areas tend to be recovered smoothly. However, the sharpness of the bump tends to get lost instead.

As observed above, k controls the trade-off between sharpness and smoothness of the recovered profile. Although recovering sharp edges from over-smoothed images is a hard task, smoothing noisy images without losing sharp edges is made possible by, e.g., the *median filter*. Here, as post-processing, we apply the median filter to the recovered surface by the LMF algorithm. More precisely, as the median of w successive output values $\{\widehat{\phi}(x+i)\}_{i=0}^{w-1}$ of the LMF algorithm, an estimate of the phase $\phi(x + (w-1)/2)$ is obtained.

The results are shown in Figure 3-(d)–(i), where w denotes the width of the median filter; $w = 1$ corresponds to the cases without the median filter. The figure shows that, as the width of the median filter increases, the surface becomes smooth while shape edges are still preserved. For this target object, $(k, w) = (2, 20)$ seems to work well. The results also show that the performance is not so sensitive to the small change in k and w. Therefore, in practice, choosing an appropriate value of k and w may not be so hard.

Figure 1-(b)–(d) depict the recovered two-dimensional surface profiles when $(k, w) = (2, 1)$, $(10, 1)$, and $(2, 20)$. For obtaining the two-dimensional surfaces, we simply applied

[1]See `http://www.cable-net.ne.jp/corp/torayins/SP-500.html` for detail.

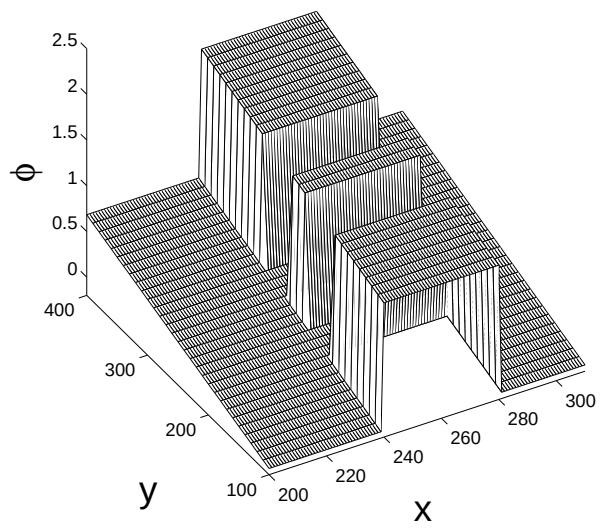

(a) Target object (Illustration)

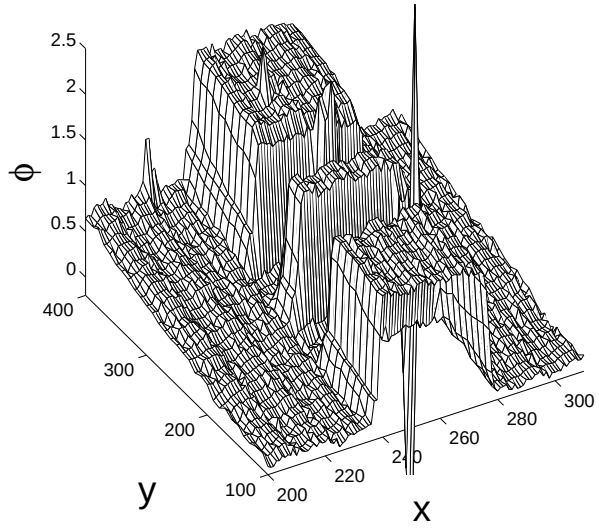

(b) Recovered with $k = 2$ and $w = 1$

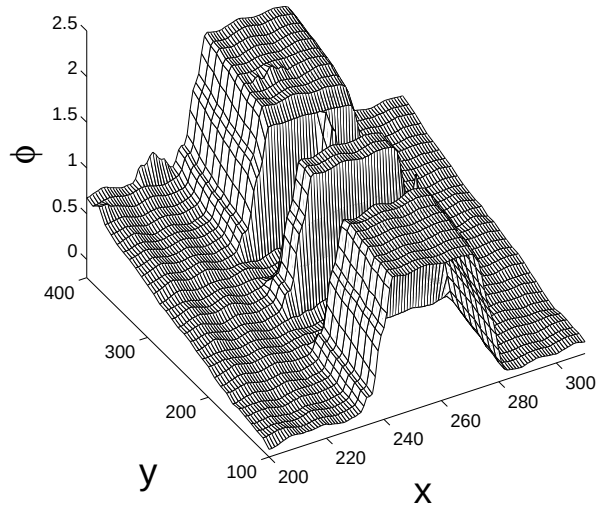

(c) Recovered with $k = 10$ and $w = 1$

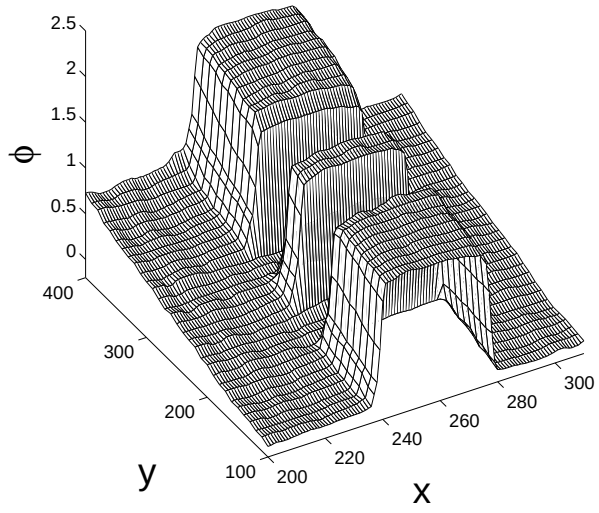

(d) Recovered with $k = 2$ and $w = 20$

Figure 1: Target and recovered surface profiles.

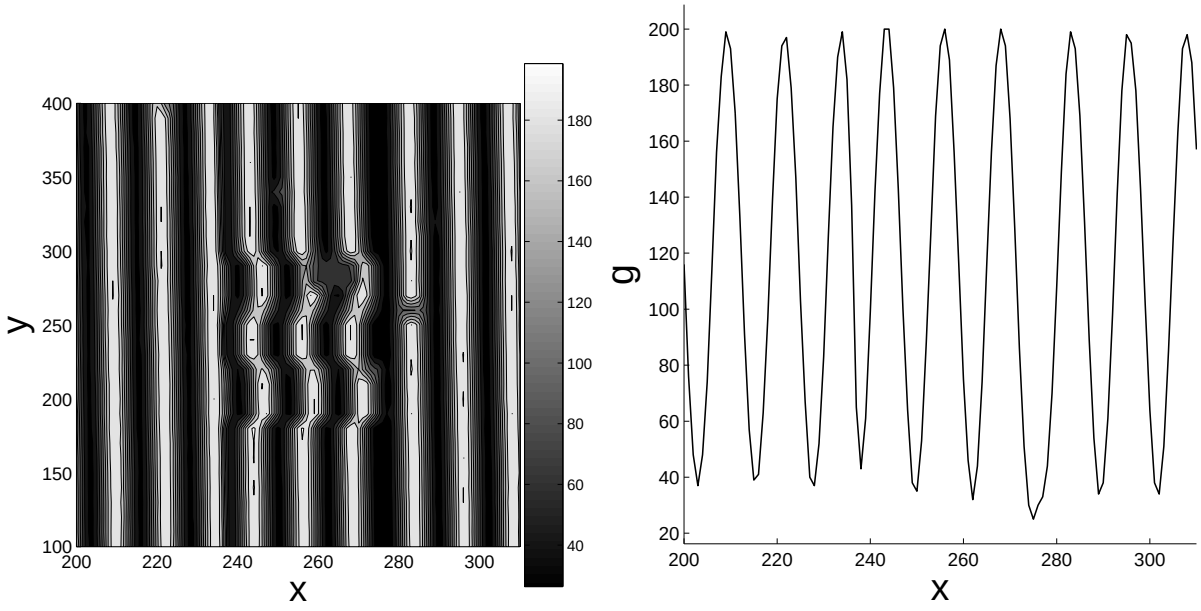

(a) $g(x, y)$ (b) $g(x, 240)$

Figure 2: Observed signal.

the above line-wise algorithm to each line independently. The recovered profiles show that $(k, w) = (2, 20)$ works excellently.

5 Conclusions

In this paper, we proposed a new surface profiling algorithm called the local model fitting (LMF) method. The LMF method is a single-shot method which requires only single image data. Therefore, it is fast and robust against disturbance such as vibration. The LMF method does not assume smoothness of the surface in the band-limit sense. This allows us to measure the surface profile of objects with sharp steps. Furthermore, the LMF method employs only local image data. Thanks to the locality, it is applicable to objects covered with heterogeneous materials. Finally, the LMF method can be implemented in a simple way, and provide a computationally efficient measurement system. Results of actual measurement showed that the LMF method followed by median filtering works excellently.

A potential weakness of the LMF algorithm could be that it may not be robust against *outliers* since least-squares fitting is heavily affected by outliers. However, since local models are used in the LMF algorithm, the effect of outliers stays only within local regions, not propagated globally. This would be an advantage of our method over existing methods [3, 4]. To improve the robustness against outliers, we may use robust statistical techniques such as *Huber's method* [8], which can systematically suppress the effect of outliers. However, this in turn increases the computational cost. Given that the effect of

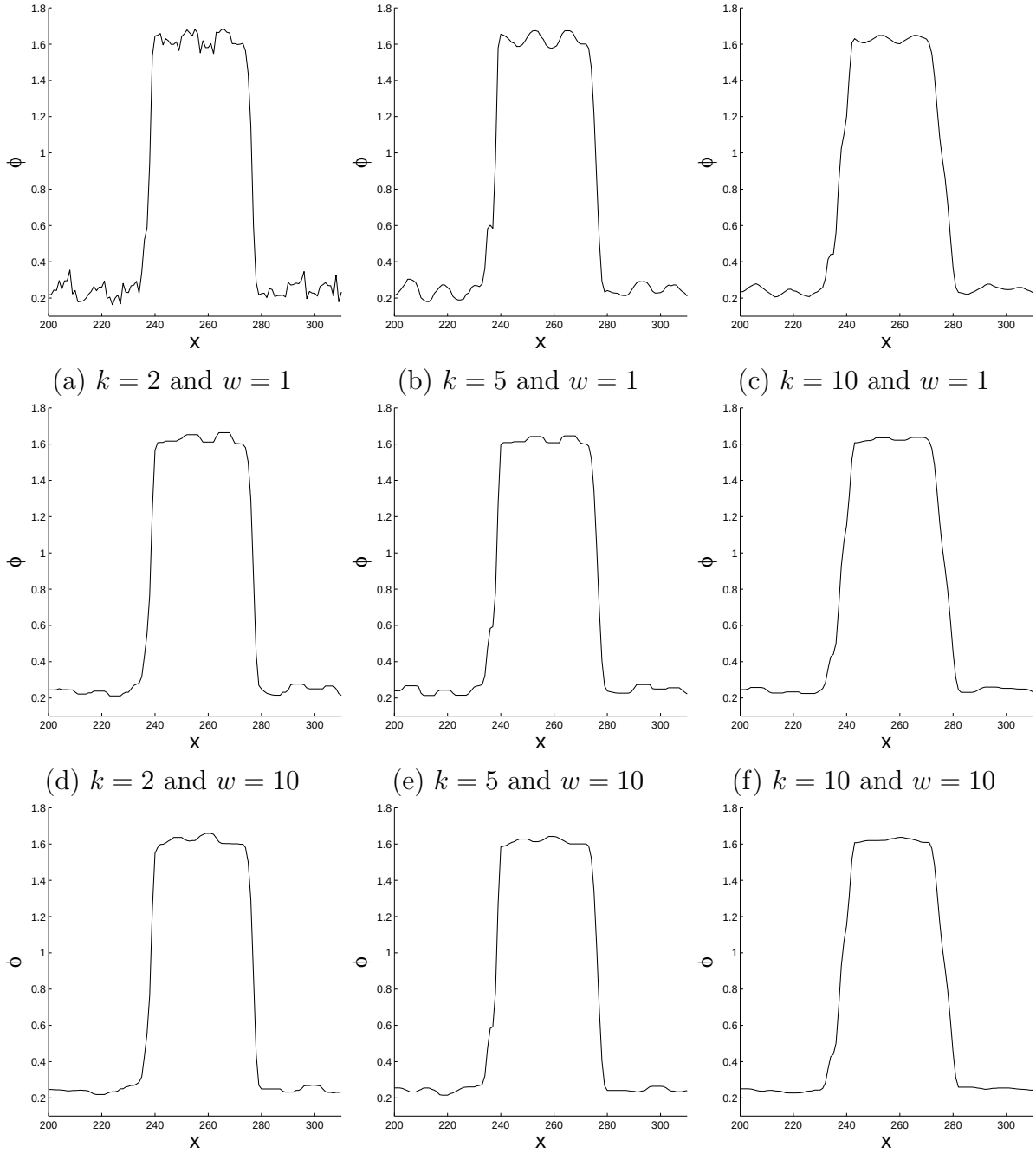

(a) $k = 2$ and $w = 1$ (b) $k = 5$ and $w = 1$ (c) $k = 10$ and $w = 1$

(d) $k = 2$ and $w = 10$ (e) $k = 5$ and $w = 10$ (f) $k = 10$ and $w = 10$

(g) $k = 2$ and $w = 20$ (h) $k = 5$ and $w = 20$ (i) $k = 10$ and $w = 20$

Figure 3: Recovered surface profiles at $y = 240$.

outliers may be weakened or removed by post-processing thanks to the locality, we think that the current form of the LMF algorithm with least-squares fitting would be practically more advantageous.

In existing global single-shot methods such as the Fourier transform method [3] and the spatial phase synchronization method [4], denoising process is *implicitly* included in the estimation process; noise is removed through low-pass/high-pass filtering where the cut-off frequency is determined from the spacial carrier frequency. This means that we can not change the cut-off frequency as desired, which limits the control of denoising capability. On the other hand, in the proposed method, denoising can be explicitly carried out as post-processing (or even pre-processing); we employed the median filter in our measurement experiments. However, it is important to note that the choice is not limited to the median filter; *any* sophisticated denoising filters can be used for denoising. Future work includes the choice of better filters depending on the type of target objects.

Acknowledgments

The authors would like to thank Minako Yokokawa and Yasushi Hidaka for their fruitful discussions. Our gratitude also goes to anonymous reviewers for their useful comments.

References

[1] J. H. Brunning, D. R. Herriott, J. E. Gallagher, D. P. Rosenfeld, A. D. White, and D. J. Brangaccio, "Digital Wave Front Measuring interferometer for Testing Optical Surface and Lenses," Applied Optics **13**(11), 2693–2703 (1974).

[2] M. Takeda and T. Abe, "Phase Unwrapping by a Maximum Cross-Amplitude Spanning Tree Algorithm: A Comparative Study," Optical Engineering **35**(8), 2345–2351 (1996).

[3] M. Takeda, H. Ina, and S. Kobayashi, "Fourier-Transform Method of Fringe-Pattern Analysis for Computer-Based Topography and Interferometry," Journal of Optical Society of America **72**(1), 156–160 (1982).

[4] J. Kato, I. Yamaguchi, T. Nakamura, and S. Kuwashima, "Video-Rate Fringe Analyzer Based on Phase-Shifting Electronic Moiré Patterns," Applied Optics **36**(32), 8403–8412 (1997).

[5] D. C. Williams, N. S. Nassar, J. E. Banyard, and M. S. Virdee, "Digital Phase-Step Interferometry: A Simplified Approach," Optics & Laser Technology **23**(3), 147–150 (1991).

[6] N. Brock, J. Hayes, B. Kimbrough, J. Millerd, M. North-Morris, M. Novak, and J. C. Wyant, "Dynamic Interferometry," in *Novel Optical Systems Design and Optimization*

VIII, Proceedings of SPIE, J. M. Sasián, R. J. Koshel, and R. C. Juergens, eds., vol. 5875, pp. 1–10 (2005).

[7] C. J. Morgan, "Least-Squares Estimation in Phase-Measurement Interferometry," Optics Letters **7**(8), 368–370 (1982).

[8] P. J. Huber, *Robust Statistics* (Wiley, New York, 1981).